Exp Brain Res (2007) 179:313–323
DOI 10.1007/s00221-006-0788-9

RESEARCH ARTICLE

Optimal inference explains dimension-specific contractions of spatial perception

Matthias Niemeier · J. Douglas Crawford · Douglas B. Tweed

Received: 7 July 2006 / Accepted: 31 October 2006 / Published online: 28 November 2006

Abstract It is known that people misperceive scenes they see during rapid eye movements called saccades. It has been suggested that some of these misperceptions could be an artifact of neurophysiological processes related to the internal remapping of spatial coordinates during saccades. Alternatively, we have recently suggested, based on a computational model, that transsaccadic misperceptions result from optimal inference. As one of the properties of the model, sudden object displacements that occur in sync with a saccade should be perceived as contracted in a non-linear fashion. To explore this model property, here we use computer simulations and psychophysical methods first to test how robust the model is to close-to-optimal approximations and second to test two model predictions: (a) contracted transsaccadic perception should be dimension-specific with more contraction for jumps parallel to the saccade than orthogonal to it, and (b) contraction should rise as a function of visuomotor noise. Our results are consistent with these predictions. They support the idea that human transsaccadic integration is governed by close-to-optimal inference.

Keywords Saccadic eye movements · Bayesian method · Space perception

M. Niemeier (✉)
Centre for Computational Cognitive Neuroscience, Department of Life Sciences, University of Toronto at Scarborough, 1265 Military Trail, M1C 1A4 Toronto, Canada
e-mail: niemeier@utsc.utoronto.ca

M. Niemeier · J. D. Crawford · D. B. Tweed
Centre for Vision Research, York University, Toronto, Canada

J. D. Crawford
Departments of Psychology, Biology, and Kinesiology, Health Sciences, York University, Toronto, Canada

D. B. Tweed
Department of Physiology, University of Toronto, Toronto, Canada

M. Niemeier · J. D. Crawford · D. B. Tweed
CIHR Group for Action and Perception, London, Canada

Introduction

Every day we make tens of thousands of saccadic eye movements that rotate the foveas of our eyes to selected objects in the visual field. This improves resolution for the foveated objects. But at the same time saccades disrupt the continuous stream of vision: reaching speeds of 700°/s, they make it difficult to extract useful visual information during the movement (Burr et al. 1982; Shiori and Cavanagh 1989; Ilg and Hoffmann 1993; Burr et al. 1994). Moreover, saccades are associated with a noisy extraretinal signal (Dassonville et al. 1992; Harris 1995), which complicates the task of tracking the spatial changes in the retinal images. To join together pre- and post-saccadic images into a unified visual percept the brain uses a process called transsaccadic integration (Hayhoe et al. 1991; Melcher and Morrone 2003; Prime et al. 2006). However, this process is imperfect: for example our ability to perceive spatial relations as constant is limited. One way to show this limited spatial constancy is to flash stimuli perisaccadically (during or just before saccades). The locations of these flashes are misperceived (e.g., Matin and Pearce 1965; Honda 1993; Cai et al.

1997), often compressed towards the saccade target (Ross et al. 1997; Morrone et al. 1997; Lappe et al. 2000; Ross et al. 2001).

It has been argued that spatial constancy is limited due to the shifts in receptive fields that neurons show around the time of a saccade (e.g., Ross et al. 2001; VanRullen 2004). These shifts are thought to reflect recoding or remapping mechanisms of spatial coordinates to anticipate the spatial changes of an impending saccade (e.g., Duhamel et al. 1992; Walker et al. 1995; Tolias et al. 2001; Nakamura and Colby 2002; Krekelberg et al. 2003). This line of reasoning would suggest that spatial constancy is affected simply by a non-specific artifact of spatio-temporal errors in the underlying neurophysiology.

Alternatively, limited spatial constancy could be a specific consequence of optimized sensorimotor integration. This seems to be the case for saccadic suppression of displacement (SSD), which is our poor perception of object displacements that occur in sync with a saccade (Mack 1970; Bridgeman et al. 1975). Though SSD is different from perisaccadic misperception of single flash locations as it requires transsaccadic comparisons of stimulus locations, it relies on similar sources of sensory information and it relates to the same perceptual problem of spatial constancy.

We have recently shown that SSD results from optimal inference given that it (a) relies on noisy sensory signals and (b) works on the normally sound assumption that stationary objects seldom jump exactly during saccades (Niemeier et al. 2003). Simulations based on these two principles correctly predicted that SSD is more prominent for the dimension parallel to the saccade than orthogonal to it and that it rises as a function of noise in the visuomotor system. What is more, our simulations also indicated that SSD is due to a new form of non-linearly contracted perception of object displacements with a range of maximum contraction for small displacements. The same kind of non-linear contractions we found in human observers. Our data suggest that some forms of misperception associated with spatial constancy are a consequence of optimal inference.

However, it is likely that human perception is merely an approximation of the optimal performance of the model, not identical to it. At present it is unclear how susceptible the model predictions are to such approximations. Even if the contractions that we observed empirically are similar to the theoretical ones, this might be coincidental. Not only neurophysiological artifacts could have caused the contractions, as another explanation, our participants might have used a task-specific response strategy. We asked participants after each saccade to reproduce the size and direction of the transsaccadic displacement by moving the object back to what they perceived as its presaccadic location. But for small object displacements the participants might have been too uncertain to do so and might have left the object on its postsaccadic location. So what appeared to be ranges of maximum contraction could simply have been a failure to respond—unlike our results for SSD for which we used a two-alternative forced-choice paradigm that does not allow nil responses. However, neither nil responses nor neurophysiological artifacts would cause transsaccadic contractions to be related to visuomotor noise.

Here we present new computer simulations and experimental data to show that our model of transsaccadic integration is robust to certain deviations from optimal. Also, we show that the model correctly predicts dimension-specific contracted transsaccadic perception and that the ranges of maximum contraction vary as a function of visuomotor noise much like SSD. Our results further support the idea that misperceptions associated with spatial constancy are due to optimal inference rather than non-specific neurophysiological artifacts.

Methods

Model simulations

For a full account of the model please refer to Niemeier et al. (2003). Briefly, the visuomotor model calculates the optimal percept of the jump of an object, called j^*. That is, it determines the percept that will yield the smallest misjudgment of the real jump (j) on average. Given there are no additional visual landmarks available, the system has three inputs that represent all available signal sources about the jump: r is retinal information about the change of the object's location in retinal coordinates before and after the saccade (i.e., a mix of object jump and eye movement); v is a similar but independent estimate of that change integrated from velocity detectors; c is the estimated change in eye position, conveyed by an extraretinal signal (in the following referred to as an 'eye position signal'). These signals are influenced by two other variables, the visuomotor system's saccades (s) and object jumps (j). From c, r and v, the system estimates j. It can be shown that the optimal estimate is:

$$j* = \int \mathrm{d}j\, j \int \mathrm{d}s\, p(s)\, p(j)\, p(c|s)\, p(r|js)\, p(v|js) / \int \mathrm{d}j \int \mathrm{d}s\, p(s)\, p(j)\, p(c|s)\, p(r|js)\, p(v|js)$$

$p(s)$ is the probability density function representing the system's prior knowledge about amplitude and direction of saccades in a given situation. For example, in our experiment, most saccade amplitudes were close to 15°. $p(j)$ is the prior probability that the object jumps in sync with the saccade—a distribution small away from zero because jumps of an otherwise stationary stimulus are unlikely. The other probability densities are conditional because c, the extraretinal signal, depends on the saccade, $p(c|s)$, and r and v, the retinal sources of information about object changes, depend on the saccade and the object jump, $p(r|js)$ and $p(v|js)$. In the simulations probability densities are modeled as Gaussians with standard deviations representing realistic noise as far as known (for details please cf. Niemeier et al. 2003). The prior for jumps, $p(j)$, is difficult to estimate because it should depend on a combination of the individual's life-time experience with object motion and probably on genetic factors. We reasoned, however, that the prior should approximate a Laplacian, given that the visuomotor system is perfectly adapted to an environment in which jumps of otherwise stationary objects are rare events whose probabilities vary across a range of different situations. For instance, when viewing a tree in a storm the prior for jumps or motion is much wider than when looking at a brick wall, and the average across a range of such individual priors (Gaussians or other unimodal functions centred on zero) approximates a Laplacian distribution.

To illustrate the model's inferences Fig. 1a shows a situation in which the visuomotor system has made a saccade 15° rightward (black curved arrow) while at the same time the saccade target, T, jumped 5° rightward (grey arrow). Therefore, in Fig. 1b the extraretinal signal, c, reports a rightward saccade of 15°, and the retinal information, r, indicates that the target has moved 10° leftward on the retina. Both signals are noisy as represented by Gaussians. Together this information implies that the target has jumped $r + c = 5°$. However, the prior probability of a jump, j, suggests that jumps of an otherwise stationary stimulus are very unlikely. The a priori information, j, and the sensorimotor information $r + c$ are integrated in the fashion of a 'tug of war' in which the optimal percept, $j*$, is 'pulled' away from $r + c$ towards j (i.e., zero). The degree of pull depends on the widths of the c, r and j distributions (note that in a situation with additional visual landmarks the model would be more complex, incorporating additional sources of visual information

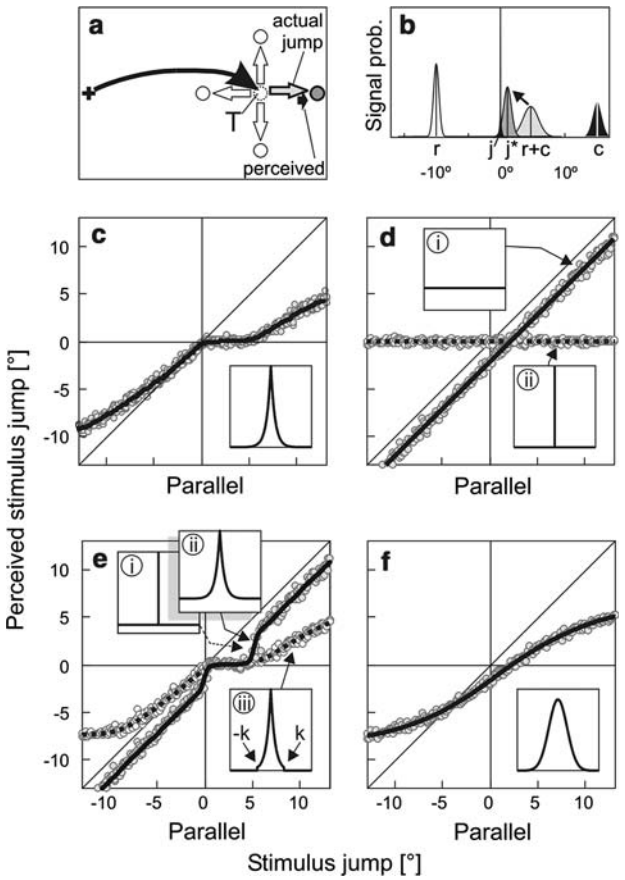

Fig. 1 Influence of prior probability density functions on $j*$-curves as predicted by the optimal inference model. **a** The model performs a saccade (*curved arrow*) 15° rightward while at the same time the saccade target (*T*) jumps 5° rightward (*grey arrow*; *white arrows* denote other possible jump directions). The optimal percept underestimates the jump (*black arrow*). **b** Signals integrated by the optimal inference model. The percept $j*$ reflects a 'tug of war' between the prior probability of a jump, j, and the sensorimotor estimate $r + c$, where r is the retinal signal and c is the efference copy signal; during saccades, v (an independent estimate of change in retinal location integrated from visual velocity detectors) has no role. *Signal prob.* signal probability. **c–f** Size and direction of stimulus jumps perceived transsaccadically are plotted as a function of the actual jumps. *Positive values* indicate jumps in saccade direction, *negative values* indicate jumps in the opposite direction. **c** $j*$-curve of the Laplacian model. The model's prior probability for jumps is a Laplacian distribution (see inset). **d** $j*$-curves of the uniform model (*solid curve*, *grey-filled circles*, inset (*i*)) and of the spike model (*dotted line*, *open circles*, inset (*ii*)). **e** $j*$-curves of the Laplacian + uniform model (*solid curve*, *grey-filled circles*, inset (*ii*)) and of the truncated Laplacian model (*dotted curve*, *open circles*, inset (*iii*)). The $j*$-curve of the third model (spike + uniform, inset (*i*)) are not presented but they look very similar to the solid curve. **f** $j*$-curve of Gaussian model. All curves are shifted owing to the delay in the extraretinal signal

about landmarks that would further reduce SSD, e.g., Deubel 2004).

We implemented the model on a computer, replacing probability densities by discrete probabilities and approximating integrals numerically. The eye position signal was set to just 0.7 of true eye position because these signals are slightly delayed and so immediately after the saccade they underestimate the size of the eye movement (Honda 1997). Finally, we added Gaussian noise to j^* to account for variance in the neural representation of the estimate.

We conducted a series of virtual SSD experiments in which our simulated visuomotor system made simulated saccades toward a target object 15° away from a fixation point. During the saccade the object jumped, either parallel or orthogonal to the eye movement, and then afterwards the system judged the direction and amplitude of the jump.

In the first set of our simulations we explored how robust the model is to imperfect approximations of optimal performance—just like a system that is well but not perfectly adapted to its environment. Therefore, we tested how the function of the prior probability of a jump impacts the model's optimal percept (variations in the noise of the system's sensory system yield percepts that are qualitatively similar; Niemeier et al. 2003). To this end we selected a range of functions that were unimodal and symmetrically centred on zero jumps because an otherwise stationary object is unlikely to move the next instant and because there is no reason to assume that leftward jumps are more or less likely than rightward ones. Additionally, we tested a uniform prior. The equations of the functions were as follows:

$$p(j) = A\exp(-|j|/m) \quad \text{(Laplacian)} \tag{2}$$

$$p(j) = c \quad \text{(uniform distributiom)} \tag{3}$$

$$\begin{aligned} &p(j=0) = 1; \quad \text{(single spike)} \\ &p(j\neq 0) = 0 \end{aligned} \tag{4}$$

$$\begin{aligned} &p(j=0) = a; \quad \text{(spike + uniform)} \\ &p(j\neq 0) = b;\ a >> b \end{aligned} \tag{5}$$

$$p(j) = A\exp(-|j|/m) + c \quad \text{(Laplacian + uniform)} \tag{6}$$

$$\begin{aligned} &p(|j|<k) = A\exp(-|j|/m);\ \text{(truncated Laplacian)} \\ &p(|j|\geq k) = 0 \end{aligned} \tag{7}$$

$$p(j) = A\exp\left(-j^2/m\right) \quad \text{(Gaussian)} \tag{8}$$

In a second set of simulations we used a Laplacian function for $p(j)$ as the one that best models a real world situation. To obtain data for different virtual observers we varied the accuracy of the model's eye position signal. The results were then compared to empirical data.

Human observers

Five subjects (three females, median age 29) gave their informed and written consent to participate in the experiment. All procedures were approved by the York University Human Participants Review Sub-Committee and have therefore been performed in accordance with the ethical standards laid down in the 1964 Declaration of Helsinki. Subjects had normal or corrected-to-normal vision. Four of them were naïve with regard to the purpose of the experiment; one was an author (MN). Four subjects participated in two or three experimental sessions, one subject (S4) participated in one. Data for parallel jumps of three subjects (S2–S4) have been reported previously (Niemeier et al. 2003).

Apparatus

Subjects sat in a dark room with their head stabilized with a bite-bar in front of a screen spanning about 100° horizontally and 90° vertically. Onto the screen an LCD projector (NEC VT540, spatial resolution 1,024 × 768 pixels, temporal resolution 72 Hz, visual decay rate < 5 ms, i/o delay ~ 10 ± 5 ms) back-projected stimuli (20 cd/m^2, background 0.015 cd/m^2) that were generated by a computer and that could be changed upon detection of saccades. Therefore, another computer monitored eye position signals at a rate of 1,000 Hz using the scleral search coil technique (Robinson 1963) with two-dimensional coils (Skalar, Delft). This method allows for almost immediate detection of saccades. We defined the start of a saccade as the first moment when eye velocity exceeded 36°/s and the eye was 1.5° away from the fixation point.

Procedure

Subjects started a trial by fixating a small dot, 0.4° across, that could appear at any one of four corners of an imaginary central 10° × 10° square. In this way we ensured that subjects could not tell the direction of the target's subsequent jump by its final location relative to the midlines of the head. (However, this precaution turned out to be unnecessary: as we tested in three

subjects, presenting the fixation spot along the horizontal meridian did not change the results).

After 0.5–1 s a target spot, 0.8° across, appeared 15° to the left or right of fixation. Subjects looked to the target as quickly as possible, and this saccade was used as a trigger to remove the fixation spot and displace the target. Jumps either parallel or orthogonal to saccade direction were tested in separate blocks of trials, and jump amplitudes were randomly chosen. Two hundred milliseconds after the jump the target turned into a mouse cursor of identical shape that the subject could move along the same dimension as the jump, horizontally or vertically, to what he or she felt was the target's presaccadic location. Subjects then clicked a mouse key upon which the screen went white for 500 ms to reduce dark adaptation and the coordinates of the mouse cursor were recorded to estimate transsaccadic jump perception (postsaccadic target location – mouse coordinates).

Results

Figure 1c–f shows the simulated visuomotor system's estimate of the target jump j^*, as a function of the true size and direction of the jump. Each data point represents the model response for one trial, and superimposed is the average j^*-curve. The insets in the panels indicate the shape of the prior probability density function for jumps, $p(j)$, that we used for the respective model simulation.

The simulation in Fig. 1c used a Laplacian for $p(j)$ (see Methods, Eq. 2; inset in Fig. 1c; note that the scale of the inset is smaller than the scale of the figure). As we have demonstrated before (Niemeier et al. 2003) this results in non-linear contraction of estimated jumps. Also, the j^*-curve (just like the curves in Fig. 1d–f) is shifted rightward (in the direction of the saccade) mostly because the system's eye position signal underestimated the saccade amplitude immediately after the saccade. Another reason is that the average saccade undershoots the target so that forward jumps, more than backward jumps, move the image of the target further away from the fovea. But this factor played only a minor role. Most remarkably, for small jumps the j^*-curve exhibits a range of maximum contraction in which jumps are perceived as greatly reduced in amplitude or even missed entirely, and about the same kind of contraction we found in human observers (Niemeier et al. 2003).

The shape of the j^*-curve is importantly influenced by the shape of the prior probability density function for jumps: the simulation in Fig. 1d considers the simplest case. That is, the prior for jumps is a uniform distribution, which means that the model regards all jump sizes and directions as equally likely (or mathematically equivalent: the model does not take information about the a priori probability of displacements into account; Eq. 3; inset (i) in Fig. 1d). This yields a linear j^*-curve with a slope of one (solid line, grey-filled circles). The model's perception is veridical except for the forward shift of the curve, though it is still prone to errors because of errors in its sensory inputs.

Exactly opposite to a uniform prior would be a single spike for zero jumps, equivalent to regarding all jumps other than zero jumps as impossible [Eq. 4; inset (ii) in Fig. 1d]. In that case the j^*-curve is entirely flat showing complete contraction because the model ignores all sensory information (dotted function, open circles in Fig. 1d).

Neither a uniform nor a spike-like prior is realistic. However, when merged [Eq. 5; inset (i) Fig. 1e] the resulting j^*-curve combines properties of those in Fig. 1d in a way that is qualitatively similar to the curve of the Laplacian model: for smaller jumps the curve runs horizontally and for larger ones it switches into a linear function with slope one while the points of transition depend on the height of the spike relative to the rest of the function (simulation results, not presented here, are very similar to the solid curve in Fig. 1e).

The prior in Fig. 1e(i) is a poor approximation of a Laplacian. More conceivable would be a prior that closely approximates a Laplacian for small jumps but deviates from it for large jumps because those are rare events with less need for approximation. One possibility would be that the probability of large jumps is overestimated. In that case the prior is similar to a Laplacian merged with a uniform function [Eq. 6; inset (ii) in Fig. 1e], and the respective j^*-curve follows the Laplacian model for small jumps and switches to the linear function of the uniform model for larger jumps (solid line, grey-filled circles, Fig. 1e). Again, the points of transition between the two models depend on the ratio of the Laplacian component relative the uniform component, not all of which may be realistic.

Alternatively, the imperfect approximation of the Laplacian could underestimate large jumps in probability. For example, the Laplacian could be truncated for jumps larger than some size k [Eq. 7; Fig. 1e, inset (iii)]. Here we truncated the Laplacian at $k = \pm 7.5°$ and obtained a j^*-curve that is identical to the curve of the Laplacian model for smaller jumps but, depending on k, for larger jumps the curve bends into horizontal lines (dotted function, open circles in Fig. 1e).

Finally, we tested the case that the model's prior is a Gaussian (Eq. 8; inset in Fig. 1f), equivalent to that of a visuomotor system that is adapted to a single type of environment in which the likelihood of motion or jumps never changes (note that this would be an artificial environment). The resulting *j**-curve is sigmoidal and its slope rises with the width of the Gaussian. Other bell-shaped priors [e.g., $p(j) = A \exp(-x^4/m)$] also yield sigmoid functions. For none of these models we found a range of maximum contraction.

Together the simulations suggest that the predictions of the transsaccadic integration model are relatively robust across a certain range of approximations of the optimal model. This makes it feasible that *j**-curves measured empirically will show properties, in particular ranges of maximum contraction of jump perception, that liken those of theoretical *j**-curves.

To directly test whether human transsaccadic perception shows the same kind of non-linear contractions, in a second set of simulations we generated specific model predictions that we then tested experimentally. First, we varied the accuracy of the model's eye position signal so as to mimic subjects with different degrees of noise in their oculomotor control. With increasing noise the *j**-curve becomes more contracted and the range of maximum contraction expands (Fig. 1a vs. b).

What is more, we found that the contractions are dimension-specific. Parallel jump estimates are more contracted with a larger range of maximum contraction than orthogonal ones because the model's eye position signal is less accurate parallel to the saccade than orthogonal to it (Fig. 1a vs. c) consistent with what is found for human extraretinal signals (Niemeier et al. 2003).

Does human transsaccadic perception of displacements follow these predictions? Figure 2 presents the data from each of our human observers individually (Fig. 3a–j) and as group means (Fig. 3k, l). To compute the average *j**-curves of jump perception we used gliding medians: we divided the data into 15 bins to calculate medians and repeated this 14 more times with bin borders that shifted by 1/15 of the bin width with each repetition. Finally, we smoothed the data with a gliding average that incorporated six neighbouring values left and right of each data point. Despite individual variations, the resulting curves are qualitatively similar to the *j**-curves of the model in that they are non-linearly contracted (though, one subject showed only slight contractions for orthogonal jumps, Fig. 3h). Also, at least four subjects (Fig. 3a, c, e, i) showed a shift of their parallel *j**-curve in the direction of the saccade. According to the model results this is mainly due to a delayed eye position signal. The same subjects showed another asymmetry in their orthogonal *j**-curves (Fig. 3b, d, f, j): their responses were less accurate for downward jumps than for upward jumps. Possible explanations for this asymmetry will be considered in the Discussion.

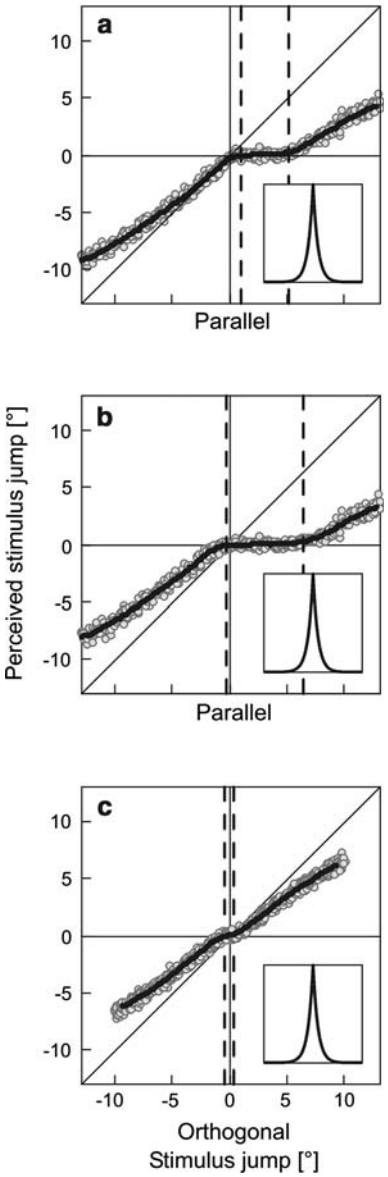

Fig. 2 Influence of extraretinal noise and of displacement direction on predicted *j**-curves. **a** Perception of jumps parallel to the saccade—in the same or the opposite direction (positive and negative values, respectively). **b** Parallel jump perception for a model with increased extraretinal noise. **c** Perception of jumps orthogonal to the saccade. *Negative values* indicate downward displacements, *positive values* are upward displacements

One major finding was that all five subjects had more contracted curves for parallel (Fig. 3a, c, e, g, i) than for orthogonal jumps (Fig. 3b, d, f, h, j). To confirm this quantitatively, we determined the ranges in

which the *j**-curves were maximally contracted, i.e., where their slopes were minimal. If the empirical contractions result from (close to) optimal transsaccadic integration this should be a measure quite sensitive to visuomotor noise (Fig. 2). We fit a spline with three linear segments to the data to find the nodes that joined together the three best fitting line segments (the dashed vertical lines in Figs. 2, 3, 4a), and we used the distance between the nodes to determine the range of maximum contraction. As predicted, that range was larger for parallel than for orthogonal *j**-curves (Fig. 4b; $t(4) = 6.22$, $P = 0.003$).

The model also predicts that jump perception during saccades should contract more with more noise in the visuomotor system. This noise cannot be observed directly so we estimated parallel versus orthogonal noise ratios from the parallel versus orthogonal scatter of saccade landing positions aimed at the target (Niemeier et al. 2003; Fig. 5). Using the data from Figs. 4b and 5b we found that scatter ratios across subjects were highly correlated with ratios of contracted jump perception ($r = 0.895$, $P = 0.040$; Fig. 6a), as predicted by the model. Furthermore, when we computed the same ratios for the model data the regression function was very similar to that of the empirical data, even though we did not fit any model parameters to the data (Fig. 6b).

Discussion

Using computer simulations we have shown that a visuomotor system exhibits contracted transsaccadic perception of displacements that is reasonably robust within a certain range of approximations to optimal inference given that the system is adapted to an environment with real-world statistics for rare events with probabilities that vary across different situations. Further we have demonstrated that the visuomotor system misperceives object motion during saccades in a dimension-specific way: the model perceived more pronounced contractions for the dimension parallel to the saccade than orthogonal to it because extraretinal signals are noisier in the parallel direction. For the same reason the amount of contraction increased when we turned up the visuomotor noise in the model. We confirmed the predictions empirically: our human observers showed similar non-linear contractions with the same difference between the dimensions parallel and orthogonal to the saccade. Moreover, we found that contracted perception was positively correlated with saccade scatter—our measure of visuomotor noise—as also predicted by the model.

These results add to our understanding of transsaccadic integration. We have recently provided evidence that visuomotor noise causes SSD, and in simulations optimal inference showed SSD due to contracted perception (Niemeier et al. 2003). Human perception, however, does not necessarily work in the same way because practically it can only be an approximation of optimal inference. In the current study we have found that a sub-optimal visuomotor system that perfectly integrates all its sensory information but disregards prior probabilities of jumps would perceive jumps veridically (Fig. 1d, solid line)—even if it still showed SSD because the sensory input is noisier during a saccade than during fixation. The results from all of our subjects now suggest that human perception is not veridical but non-linearly contracted for the dimension parallel to the saccade as well as for the orthogonal dimension and that these contractions are difficult to explain with a failure to respond because they are correlated with visuomotor noise. Instead, the contractions are similar to those predicted by the versions of our model that use or approximate a Laplacian prior for displacements, suggesting that such a prior lets human transsaccadic perception ''distrust'' its noisy sensory input. The same principles of optimal inference have been proposed to produce other kinds of contractions or misperceptions (e.g., Weiss et al. 2002) and can be easily and implicitly learned by neural networks (Niemeier et al. 2002).

Despite the empirical contractions being similar to our model predictions, they do differ in that for larger jumps the slopes of the empirical *j**-curves are steeper than those of the optimal model. We have three possible explanations. First, the empirical *j**-curves might differ due to an imperfect approximation of the priors. Second, the noise on the sensory inputs of the model might be inaccurate. Third, some of the differences might be due to pointing errors when subjects responded.

As a second difference our data suggest that downward jumps were somewhat more difficult to see than upward jumps (Fig. 3l). Is it possible that humans are less accurate at perceiving displacements into the lower visual field? The distribution of visual neurons is known to be biased towards the lower visual field (Curcio and Allen 1990; Maunsell and Newsome 1987; Maunsell and Van Essen 1987; Schein and de Monasterio 1987), which would rather suggest the opposite, higher motion sensitivity in the lower visual field. An alternative explanation could be that higher motion sensitivity results in stronger intra-saccadic suppression of motion (for now our model incorporates motion suppression but it is the same for all parts of the visual

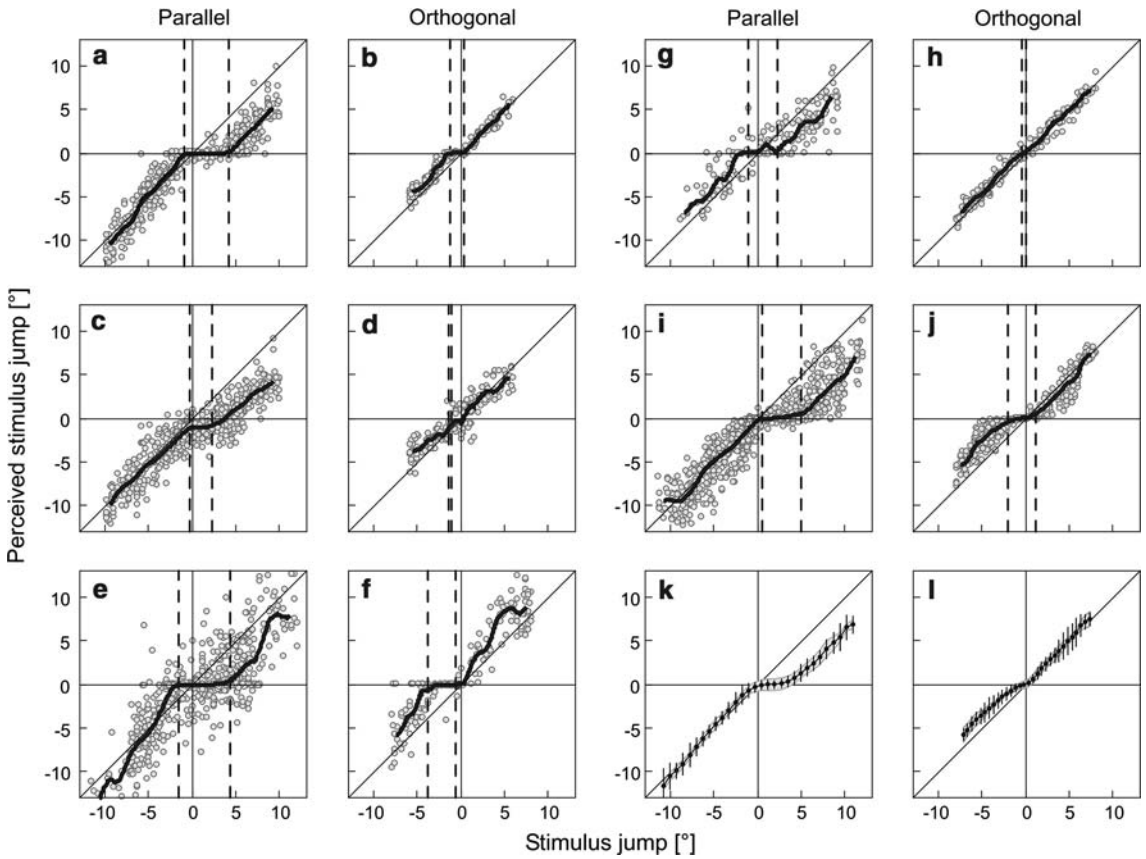

Fig. 3 *j**-Curves of five human observers. The *first* and *third column* show perception for jumps parallel to the saccade and the *second* and *fourth column* show perception for orthogonal jumps. Superimposed onto the single data points are gliding medians. *Dashed lines* mark the ranges of maximum contraction (see Fig. 4a). **a**, **b** Subject S1. **c**, **d** Subject S2. **e**, **f** Subject S3. **g**, **h** Subject S4. **i**, **j** Subject S5. **k**, **l** Group averages. *Black circles* are binwise averages of the gliding medians of the individual data sets. *Error bars* represent standard deviations for those bins, and *grey envelopes* indicate averages of the gliding standard deviations of the individual data

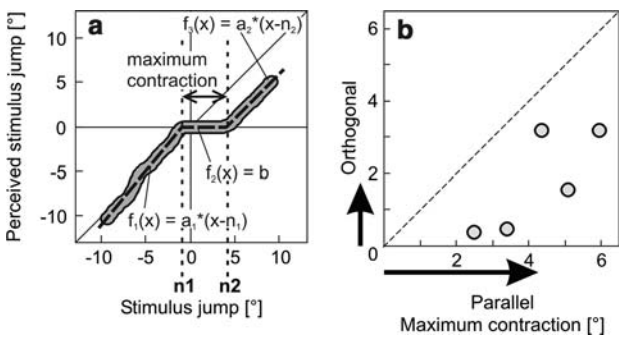

Fig. 4 Perceptual parameters. **a** A spline with three linear segments and five free parameters (*thick dashed curve*) was fit to the gliding medians (*thick grey curve*; see Fig. 3a) using a gradient descent method. The *dashed vertical lines* mark the horizontal coordinates of nodes n1 and n2 that connect the three spline segments. **b** Ranges of maximum contraction for individual subjects. Ranges for orthogonal jump perception are plotted as a function of parallel jump perception. *Arrows* indicate group averages

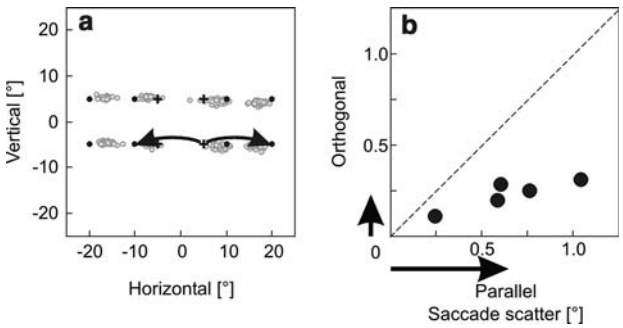

Fig. 5 Oculomotor parameters. **a** 2D plot of saccade scatter for a typical subject (S4). *Black crosses* indicate the four fixation spots. *Black circles* represent saccade targets, and *grey circles* indicate where the saccades actually landed. **b** Standard deviations of saccade scatter for individual subjects. Saccade scatter orthogonal to the saccade is plotted as a function of parallel scatter. *Arrows* indicate group averages. Parallel scatter is greater than orthogonal scatter (van Opstal and van Gisbergen 1989; $t(4) = 4.30$, $P = 0.013$)

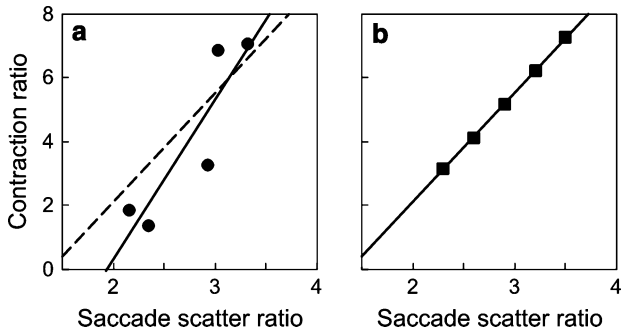

Fig. 6 Relation between perception and motor control. **a** Data from human observers. Contraction ratios are calculated from the data in Fig. 4b, and saccade scatter ratios are calculated from Fig. 5b. *Solid line* regression line, *dashed line* model prediction from **b**. We can also quantify the data, instead of with contraction ratios with contraction indices. That is, calculating (parallel – orthogonal) / (parallel + orthogonal) yields about the same high correlation ($r = 0.905$, $P = 0.035$). **b** Model data. *Black squares* represent the data for five simulated subjects with varying ratios of saccade scatter and maximum contraction ranges. Contractions were calculated in the same way as described for the human observers

field). As a third possibility, the prior for sudden vertical stimulus jumps could be asymmetric because stationary objects often rest on some surface and are less likely to move, if at all, in that direction. Which of these possibilities should be incorporated in a future version of the optimal inference model, either as modified physiological constraints or an adjustment of the priors, depends on further tests.

Nevertheless, the fact that ranges of maximum contraction in the *j**-curves should be correlated with saccade scatter is a very specific prediction of the optimal inference model that is clearly supported by our experimental data. At present we are unaware of an alternative model that could explain this correlation. Our results therefore strongly support the idea that human transsaccadic misperceptions are governed by optimal, or close-to-optimal, transsaccadic integration (Niemeier et al. 2003).

Optimal inference versus neurophysiological artifact

A central challenge in comparing our 'optimal inference' explanation of contractions as observed here with 'neurophysiological' explanations is that the former works at the 'computational level' whereas the latter works at the 'implementation level' of vision (Marr 1982). Before attempting to merge these two levels, let us first consider the previously proposed 'neurophysiological' explanations in more detail.

According to one interpretation perceptual contractions could be due to a non-optimal neural implementation of transsaccadic integration: cortical remapping or updating processes refer to a phenomenon observed in the parietal cortex, in striate, extrastriate and other areas where neurons move their receptive fields around the time of the saccade so as to anticipate the postsaccadic retinal image (Duhamel et al. 1992; Walker et al. 1995; Tolias et al. 2001; Nakamura and Colby 2002). Ross et al. (2001) have pointed out that neurons in these areas do not uniformly shift their receptive fields and so areas that calculate stimulus locations based on remapping mechanisms may actually code different locations as the same, thus resulting in shifted and compressed perception of spatial locations. This is much like the misperceptions of the locations of objects, which can occur when these objects are briefly flashed around the time of the saccade (Ross et al. 1997; Morrone et al. 1997; Lappe et al. 2000).

A related but different interpretation of such saccadic misperceptions has been offered by VanRullen (2004). He simulated a logarithmic cortical representation of space using biologically plausible parameters of cortical magnification. He then made the assumption that remapping would cause a uniform shift of reference in these cortical logarithmic coordinates and showed that this would yield a shifted and compressed representation of space. Though as yet there is no theoretical or physiological basis for the assumed uniform shift in log coordinates, VanRullen's (2004) simulated misperceptions closely resembled those reported in the literature, with little compression orthogonal to the saccade, especially between fixation point and saccade target, and much stronger compression parallel to the saccade (Kaiser and Lappe 2004; also see Morrone et al. 1997 for similar dimension-specific differences). Interestingly, a dimension-specific distribution of misperceptions is also quite similar to the dimension-specific transsaccadic contractions we have studied here, though it is important to emphasize that transsaccadic contractions (Niemeier et al. 2003) and perisaccadic compression (Ross et al. 1997; Morrone et al. 1997; Lappe et al. 2000; Kaiser and Lappe 2004) are two different perceptual phenomena obtained from different experimental paradigms. Nevertheless, in the future it will be interesting to further explore how much they have in common (e.g., both have been shown to be governed by oculomotor mechanisms; Awater et al. 2005; Niemeier et al. 2003).

Since neurophysiology-based concepts and our explanation for SSD refer to different conceptual levels (implementation vs. computation), it is possible that

they are in fact different aspects of the same process. In other words, the neurophysiological observations may be, and probably are, part of the implementation of the optimal inference process we have proposed. At least, it is possible that remapping and optimal inference are complementary rather than mutually exclusive.

However, our data reject one particular aspect of the neurophysiological explanation, i.e., that compression arises purely as an artifact of remapping. That is, the remapping theory in itself does not explain why the ratios of perceived contraction observed in the present study correlate with saccade scatter (unless remapping caused a noisy motor command that resulted in saccade scatter; but as far as is known, remapping is not an oculomotor phenomenon, i.e., it is not the motor command that drives eye movements; Duhamel et al. 1992; Walker et al. 1995; Nakamura and Colby 2002, for the same reason it is difficult to explain our data with effects of visual attention).

It is very likely that remapping, similar to other forms of distorted spatial representation (Krekelberg et al. 2003), is driven by extraretinal information about eye position. This information could be derived from an efference copy that comes up from the superior colliculus through colliculus projection areas in the thalamus (Sommer and Wurtz 2002), and such an extraretinal signal also seems to be used as a control signal in the oculomotor system (van Opstal and van Gisbergen 1989; Harris 1995; Niemeier et al. 2003), probably occurring in the superior colliculus and/or downstream in the 3D eye control centres in the brainstem (Smith and Crawford 2001; Medendorp et al. 2003). However, a noisy cortical representation of eye position alone would not yield non-linear contractions (Fig. 1d). Such contractions could be associated with cortical magnification similar to VanRullen's (2004) assumptions but then it would remain difficult to explain the correlations with saccade scatter—across different subjects. This leaves optimal inference as the most parsimonious explanation for the data.

In conclusion, our data suggest that contracted perception of saccadic displacements is well explained by a simple model of optimal inference from noisy sensorimotor signals and from a priori knowledge rather than mechanisms of cortical remapping, even though the two mechanisms are not mutually exclusive. Our study also supports the notion that a complete understanding of perception must consider the interactions between sensory and motor processes.

Acknowledgments We thank Saihong Sun, Dr. Hongying Wang and Steve Prime for technical assistance. This work was supported by CIHR.

References

Awater H, Burr D, Lappe M, Morrone MC, Goldberg ME (2005) Effect of saccadic adaptation on localization of visual targets. J Neurophysiol 26:12–20

Bridgeman B, Hendry D, Stark L (1975) Failure to detect displacement of the visual world during saccadic eye movements. Vision Res 15:719–722

Burr DC, Holt J, Johnstone JR, Ross J (1982) Selective depression of motion sensitivity during saccades. J Physiol 333:1–15

Burr DC, Morrone MC, Ross J (1994) Selective suppression of the magnocellular visual pathway during saccadic eye movements. Nature 371:511–513

Cai RH, Pouget A, Schlag-Rey M, Schlag J (1997) Perceived geometrical relationships affected by eye movement signals. Nature 386:601–604

Curcio CA, Allen KA (1990) Topography of ganglion cells in human retina. J Comp Neurol 300:5–25

Dassonville P, Schlag J, Schlag-Rey M (1992) Oculomotor localization relies on a damped representation of saccadic eye displacement in human and non-human primates. Vis Neurosci 9:261–269

Deubel H (2004) Localization of targets across saccades: role of landmark objects. Vis Cogn 11:173–202

Duhamel JR, Colby CL, Goldberg ME (1992) The updating of the representation of visual space in parietal cortex by intended eye movements. Science 255:90–92

Harris CM (1995) Does saccadic undershoot minimize saccadic flight-time? A Monte-Carlo study. Vision Res 35:691–701

Hayhoe M, Lachter J, Feldman J (1991) Integration of form across saccadic eye movements. Perception 20:393–402

Honda H (1993) Saccade-contingent displacement of the apparent position of visual stimuli flashed on a dimly illuminated structured background. Vision Res 33:709–716

Honda H (1997) Interaction of extraretinal eye position signals in a double-step saccade task: psychophysical estimation. Exp Brain Res 113:327–336

Ilg U, Hoffmann KP (1993) Motion perception during saccades. Vision Res 33:211–220

Kaiser M, Lappe M (2004) Perisaccadic mislocalization orthogonal to saccade direction. Neuron 41:293–300

Krekelberg B, Kubischik M, Hoffmann KP, Bremmer F (2003) Neural correlates of visual localization and perisaccadic mislocalization. Neuron 37:537–545

Lappe M, Awater H, Krekelberg B (2000) Postsaccadic visual references generate presaccadic compression of space. Nature 403:892–895

Mack A (1970) An investigation of the relationship between eye and retinal image movement in the perception of movement. Percept Psychophys 8:291–298

Marr D (1982) Vision. Freeman, San Francisco

Matin L, Pearce DG (1965) Visual perception of direction for stimuli flashed during voluntary saccadic eye movements. Science 148:1485–1488

Maunsell JHR, Newsome WT (1987) Visual processing in monkey extrastriate cortex. Annu Rev Neurosci 10:363–401

Maunsell JHR, Van Essen DC (1987) Topographical organization of the middle temporal visual area in the macaque monkey: representational biases and the relationship to callosal connections and myeloarchitectonic boundaries. J Comp Neurol 266:535–555

Medendorp WP, Tweed DB, Crawford JD (2003) Motion parallax is computed in the updating of human spatial memory. J Neurosci 23:8135–8142

Melcher D, Morrone MC (2003) Spatiotopic temporal integration of visual motion across saccadic eye movements. Nat Neurosci 6:877–881

Morrone MC, Ross R, Burr DC (1997) Apparent position of visual targets during real and simulated saccadic eye movements. J Neurosci 17:7941–7953

Nakamura K, Colby CL (2002) Updating of the visual representation in monkey striate and extrastriate cortex during saccades. Proc Natl Acad Sci USA 99:4026–4031

Niemeier M, Crawford JD, Tweed DB (2002) A bayesian approach to change blindness. Ann N Y Acad Sci 956:474–475

Niemeier M, Crawford JD, Tweed DB (2003) Optimal transsaccadic integration explains distorted spatial perception. Nature 422:76–79

van Opstal AJ, van Gisbergen JA (1989) Scatter in the metrics of saccades and properties of the collicular motor map. Vision Res 29:1183–1196

Prime S, Niemeier M, Crawford JD (2006) Transsaccadic integration of visual features in a line intersection task. Exp Brain Res 169:532–548

Robinson DA (1963) A method of measuring eye movement using a scleral search coil in a magnetic field. IEEE Trans Biomed Eng 10:137–145

Ross J, Morrone MC, Burr DC (1997) Compression of space before saccades. Nature 386:598–601

Ross J, Morrone MC, Goldberg ME, Burr DC (2001) Changes in visual perception at the time of saccades. Trends Neurosci 24:113–121

Schein SJ, de Monasterio FM (1987) Mapping of retinal and geniculate neurons onto striate cortex of macaque. J Neurosci 7:996–1009

Shiori S, Cavanagh P (1989) Saccadic suppression of low-level motion. Vision Res 29:915–928

Smith MA, Crawford JD (2001) Implications of ocular kinematics for the internal updating of visual space. J Neurophysiol 86:2112–2117

Sommer MA, Wurtz RH (2002) A pathway in primate brain for internal monitoring of movements. Science 296:1480–1482

Tolias AS, Moore T, Smirnakis SM, Tehovnik EJ, Siapas AG, Schiller PH (2001) Eye movements modulate visual receptive fields of V4 neurons. Neuron 29:757–767

VanRullen R (2004) A simple translation in cortical log-coordinates may account for the pattern of saccadic localization errors. Biol Cybern 91:131–137

Walker MF, Fitzgibbon EJ, Goldberg ME (1995) Neurons in the monkey superior colliculus predict the visual result of impending saccadic eye movements. J Neurophysiol 73:1988–2003

Weiss Y, Simoncelli EP, Adelson EH (2002) Motion illusions as optimal percepts. Nat Neurosci 5:598–604